

# 1 Biological Background and Experimental Motivation

To construct a conductance-based model that replicates electrophysiological findings in R5 neurons, it is essential to first understand the cellular mechanisms underlying burst generation, transition between spiking and bursting regimes, and neuronal activity following blockade of sodium channels. Which processes might modulate neuronal activity to explain the experimental findings, and what mechanisms might underlie these effects?

This section provides an overview of the literature on sleep in *Drosophila*, with a focus on R5 neurons. These neurons are thought to encode sleep drive and induce Slow-Wave Activity (SWA) during increased sleep pressure in the *Drosophila* Central Nervous System (CNS). In this section, sleep is viewed from the point of R5 neurons: Which circuits and processes modulate the activity of R5 neurons, and what are the potential underlying mechanisms at the circuit level? What is the function of R5 neurons, and how can their activity modulate other neuronal populations, as well as the behaviour of the animal? Which cellular processes might be involved in the regulation of R5 activity, together with external input from circuits that modulate R5 activity? Finally, several relevant experimental findings are discussed, along with proposed mechanisms underlying these findings.

## 1.1 Ion Channels

### 1.1.1 General Properties and Function

**Ion channels** are proteins found on the membrane of a neuron, which allow flow of ions (such as  $Na^+$ ,  $Ca^{2+}$ ,  $K$ , or  $Cl^-$ ) across the membrane and contribute to modulation of membrane potential, neuronal excitability, and synaptic transmission. For a given ion channel, the rate of the ion flow across that channel at the given moment can depend on different factors, such as membrane potential, intracellular ion concentration, or temperature. Thus, in contrast to, e.g. Integrate-and-fire (IAF) model, **conductance-based models** incorporate activity-dependent conductances and provide a biologically plausible approach that more accurately captures the shape of neuronal responses (Alain Destexhe 1997). In 1952, Hodgkin and Huxley published the first conductance-based model describing initiation of an action potential of a squid giant axon based on gating mechanisms of  $Na^+$ ,  $K^+$  and leak currents (Hodgkin and Huxley 1952),

for which they were awarded the Nobel Prize in 1963. The mechanism of bursting and transition between different activity states in R5 neurons is more complex and would require the incorporation of different ion channels in the model.

By convention, the potential in the extracellular space is defined to be 0 V and the voltage across the membrane (termed as **membrane potential**) is measured as the intracellular potential relative to the extracellular one. At rest, the potential difference across the membrane is negative, typically on the order of a few tens of millivolts. The concentration of ions also differs between the extracellular and intracellular space (for instance, the concentrations for a typical mammalian neuron are given in Table 1). Furthermore, currents that **depolarize** the membrane (i.e. positive ions entering the cell, or negative ions leaving the cell) are defined to be **positive**. Similarly, currents that **hyperpolarize** the membrane (i.e. positive ions leaving the cell, negative ions entering the cell) are defined to be **negative**.

The direction of an ion flow through a specific ion channel at any given moment depends on intra- and extracellular ion concentrations, as well as the membrane potential at that moment. Given ion concentrations, using the Nernst equation, one can compute the membrane potential for which the direction of the current is reversed (Izhikevich 2006) (**Nernst potential**, or **Reversal potential** of specific ion):

$$E_{ion} = \frac{RT}{zF} \ln \frac{[Ion]_o}{[Ion]_i} \quad (1.1)$$

where,  $R$  is the universal gas constant (8315 mJ/(K°·Mol)),  $T$  is temperature measured in Kelvin,  $F$  is Faraday's constant (96480 coulombs/Mol),  $z$  is the valence of the ion, whereas  $[Ion]_i$  and  $[Ion]_o$  are ion concentrations inside and outside membrane.

Not all channels are selective to single ion species. Some channels (e.g. ones mediating

Ion	Intracellular	Extracellular
$Na^+$	5-15 mM	145 mM
$K^+$	140 mM	5 mM
$Cl^-$	4 mM	110 mM
$Ca^{2+}$	0.1 $\mu$ M	2.5-5 mM

**Table 1: Intra- and extracellular ion concentrations for mammalian neurons.** Data taken from (Izhikevich 2006).

hyperpolarization-activated current  $I_h$ ) are permeable to multiple ions. Additionally, in models, ionic current may represent the combined effect of several ion channel types (such as  $K^+$  and  $Na^+$  leak channels). In such cases, a single reversal potential is often used (see e.g. (Wang 1994)).

Apart from the reversal potential, the magnitude of current through an ion channel depends on the gating mechanism of the channel. Ion channels may have **activation** and/or **inactivation gates** (Figure 1). Activation gates can be thought of as doors which, if open, let ions pass through the channel. Inactivation gates are the mechanisms to block the channel and act independently from the activation gates. In general, an ion channel contains at most one inactivation gate and one or more activation gates. For ions to pass through the channel, all gates must be in the open state simultaneously. Each gate is characterized by the probability of the gate to be in the open state, which can depend on membrane potential, concentration of ligands (i.e. ions or molecules that bind to the channel and influence its gating properties), temperature, or combinations of these factors. One common example of a ligand-gated ion channel is a family of  $Ca^{2+}$  gated  $K^+$  channels, in which calcium influx can either open or close the channel depending on the specific channel subtype.

Ion channels whose gating mechanism solely depends on membrane potential are referred to as **voltage-gated ion channels**. Similarly, if Channel gating depends on the presence of ligands, they are classified as **ligand-gated ion channels**. Depending on the membrane potentials at which voltage-gated ion channels are in an open state, they can modulate subthreshold membrane potential, spike shape, or both. Furthermore, the gating mechanism of some ion channels depends on both voltage and the presence of a ligand. In such cases, the channel opens only when both conditions are met.

In neuronal models, usually ion channels are not modelled explicitly. Rather, the models describe the behaviour of a population of ion channels. Thus, the flow of the current through a given channel depends on the maximum conductance (i.e. conductance when all channels are open) and the probability that the gates are in an open state.

Importantly, in response to changes in membrane voltage or ligand concentration, not all channels open or close simultaneously. Instead, transitions between open and closed states occur with a certain probability. At the population level, the probabilistic behaviour is characterized by

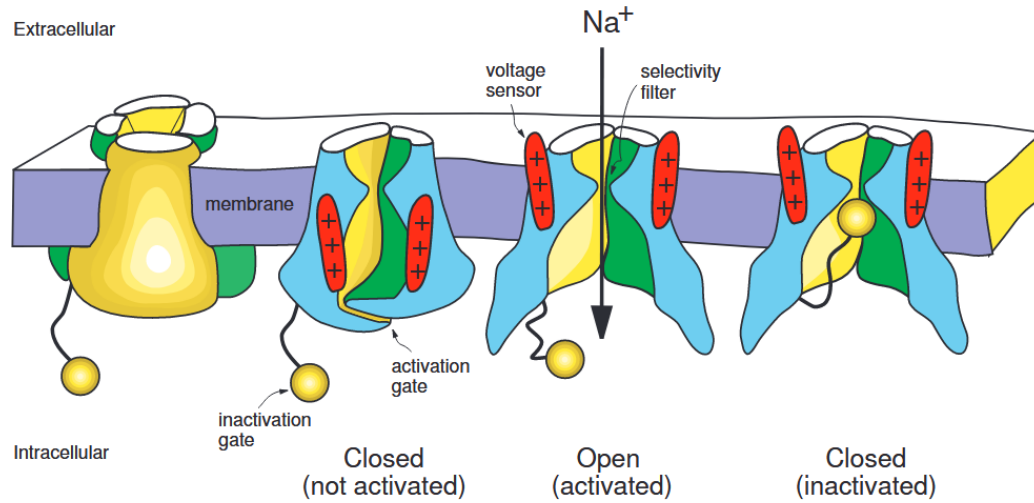


**Figure 1: Activation and inactivation gates.** The figure illustrates a typical example of a voltage-gated ion channel (here, permeable to  $Na$ ) consisting of both activation and inactivation gates. From left to right: (1) a schematic of the ion channel; (2) a cross section showing the activation gate closed and the inactivation gate open; (3) both gates open, allowing ions to pass through the ion channel; (4) the activation gate open, but the ions can not pass through the ion channel because of the blockade by the inactivation gate. Figure adapted from (Izhikevich 2006).

associated **gating time constants**. These time constants can vary depending on the channel type, ranging from several milliseconds (fast) to several seconds (slow). The mathematical description of ion channels, their gating mechanisms and how gating constants are related to the transition probabilities between open and closed states is provided in Section ??.

### 1.1.2 Known ion channels in *Drosophila* R5 neurons

There is a limited amount of literature about what types of ion channels are present in R5 neurons. To my knowledge, the only experimentally confirmed ion channel in these neurons is the **T-type  $Ca^{2+}$  ion channel**, localised at presynaptic terminals (unpublished study by David Oswald and colleagues). In many bursting models (biological as well as computational), T-type channels have been found to be important for bursting (see Section 1.3.2).

The second ion channel that potentially is present in R5 neuron is potassium **ether-à-go-go (EAG)** channel, which could potentially regulate neuronal excitability (Brüggemann et al. 1993). A recent study reported diurnal variation in the gene expression encoding the potassium EAG channel in R5 neurons of *Drosophila* (Dopp et al. 2024). Although direct evidence for

the presence of EAG channels in R5 neurons has not been reported, rhythmic modulation of the gene expression in R5 neurons, suggests that EAG may indeed be present in R5 and take part in diurnal modulation of its activity. As potassium channels are thought to decrease neuronal excitability (Brüggemann et al. 1993), and EAG was shown to be negatively correlated with R5 activity (Dopp et al. 2024), diurnal variation of EAG expression might be an important mechanism to switch R5 activity from tonic during the daytime to bursting at night.

Additionally, **voltage-gated sodium channels (DMNa<sub>v</sub>)** have been detected in *Drosophila* active neurons, suggesting that they are also expressed in R5 neurons.

Interestingly, both the T-type calcium and DMNa<sub>v</sub> channels are encoded by single genes (Jeong et al. 2015; Ravenscroft et al. 2020). *para* gene, which encodes DMNa<sub>v</sub>, has been shown to be responsible for mediating both transient and persistent components of sodium channels, likely via a process called alternative splicing (Lin et al. 2009). To my knowledge, it has never been reported whether alternative splicing applies to the genes encoding T-type and EAG channels in *Drosophila*.

## 1.2 Sleep in *Drosophila*

### 1.2.1 Circadian and Homeostatic Processes

Sleep in *Drosophila* is typically defined by a period of inactivity lasting more than 5 minutes (Dubowy and Sehgal 2017; Shafer and Keene 2021). Similar to vertebrates, in *Drosophila* sleep-wake cycle is regulated by two independent processes - circadian and homeostatic (Dopp et al. 2024; Sha Liu et al. 2016).

Circadian rhythm (circa - approximately, diem - day; also known as process C) refers to the behavioural or physiological processes that recur with a period approximately equal to 24 hours (Fernandez-Chiappe et al. 2021; Dubowy and Sehgal 2017). Its function is believed to be the regulation of the sleep-wake cycle and suppression of sleep when sleep is dangerous or unfavourable, even in case of high sleep pressure (Shafer and Keene 2021; Andreani et al. 2022). At the cellular level, it consists of transcriptional-translational feedback loops that produce ~ 24 hour period cycles in gene expression, including genes that encode ion channel proteins (Dopp et al. 2024; Dubowy and Sehgal 2017; Andreani et al. 2022).

On the other hand, homeostasis (or, process S) is thought to reflect the sleep need based on duration of wakefulness, mediated by the build-up of byproducts (e.g. Reactive Oxygen Species (ROS)) from increased neuronal activity (Suárez-Grimalt and Raccuglia 2021; Dopp et al. 2024; Andreani et al. 2022; Schmutz et al. 2014). Similar to circadian process, gene expression can also be correlated with the level of the sleep drive (Sha Liu et al. 2016). R5 neurons, originally referred to as R2 (Shafer and Keene 2021; Sha Liu et al. 2016; Donlea et al. 2018), consisting of only approximately 32 cells in the adult fly brain (Dopp et al. 2024), have been suggested to encode sleep homeostat, as plasticity of these neurons was shown to be both necessary and sufficient for generating sleep drive (Sha Liu et al. 2016; Dopp et al. 2024).

Interestingly, a recent study reported that a given cell in *Drosophila* was mostly affected by only one process - circadian or homeostatic, with the exception of glial cells, which were affected by both processes (Dopp et al. 2024).

### **1.2.2 Circuits involved in *Drosophila* sleep regulation**

The central complex in *Drosophila* brain has been shown to have a critical function in the regulation of sleep duration and homeostasis. It contains several neuron types, including helicon cells, dorsal Fan-Shaped Body (dFB), and Ellipsoid Body (EB) neurons (Shafer and Keene 2021). Generation of coherent SWA in the central complex has been strongly associated with sleep need and quality (Suárez-Grimalt and Raccuglia 2021; Raccuglia, Huang, et al. 2019). Furthermore, networks within the central complex act as a sensory gate promoting transitions between sleep and wakefulness, similar to mammalian thalamocortical (TC) neurons (Raccuglia, Suárez-Grimalt, et al. 2022; Gent et al. 2018).

Experimental observations have suggested that SWA might be generated at the level of R5, emerging via synchronous firing of individual R5 neurons at night and following sleep-deprivation (Raccuglia, Huang, et al. 2019). Studies of the previous decade have identified several circuits modulating R5 activity, sleep-wake states and arousability during sleep. The circuits involved in *Drosophila* sleep regulation are summarized in Figure 2.

The first circuit involves Dorso-posterior (DN1p) clock neurons and visually sensitive tubercular bulbar (TuBu) neurons. It represents circadian modulation of R5 neurons through DN1p neurons. TuBu neurons are sensitive to polarized light and are thought to be important for

navigation (Suárez-Grimalt and Raccuglia 2021). They provide excitatory input to R5 neurons (Duan et al. 2023). It has been demonstrated that activation of TuBu neurons increases single-unit power of R5 neurons, induces SWA in R5 and promotes sleep (Andreani et al. 2022; Raccuglia, Huang, et al. 2019). On the other hand, DN1p neurons inhibit TuBu neurons (Lamaze et al. 2018) and exhibit diurnal variation in their firing patterns (Flourakis et al. 2015). Firing rate of the DN1p neurons shows the peak of  $\sim 10$  Hz in the early morning, which is monotonically reduced until evening, when the neurons are almost silent. Afterwards, the firing rate starts to gradually increase again until the next morning (Flourakis et al. 2015). Thus, DN1p mediated inhibition of TuBu neurons during day might facilitate sensory processing, while release of inhibition in the evening may promote TuBu mediated compound SWA in R5 neurons and facilitate switch of their activity from tonic firing to bursting (see Section 1.4.2). Indeed, activation of either DN1p or TuBu neurons is sufficient to induce oscillations in R5 neurons (Suárez-Grimalt and Raccuglia 2021; Raccuglia, Huang, et al. 2019). Notably, silencing TuBu neurons did not affect the rebound sleep after sleep deprivation (Andreani et al. 2022), suggesting that they are

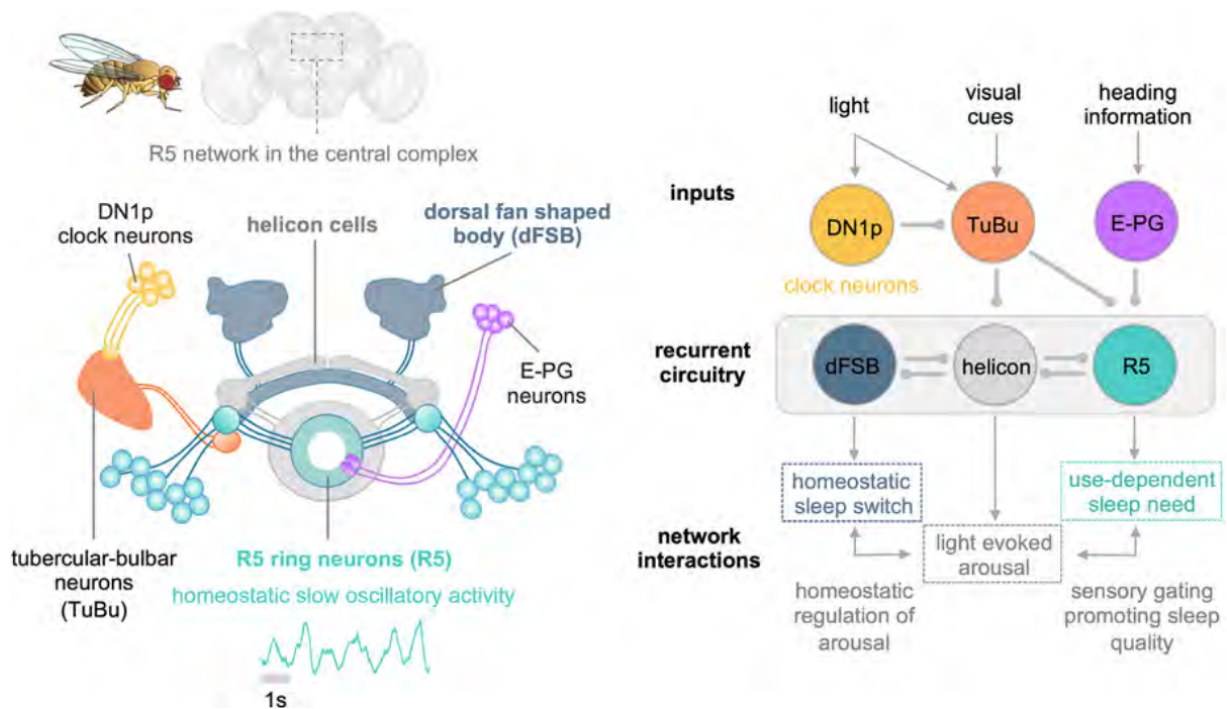


**Figure 2: Circuits involved in *Drosophila* sleep.** Left: anatomical organisation of neurons involved in sleep regulation. Right: schematic diagram of sleep-regulating network in *Drosophila* brain. Adapted from (Suárez-Grimalt and Raccuglia 2021)

not involved in homeostatic regulation of sleep.

The second circuit includes a functional connection between dFB and R5 neurons via excitatory helicon cells (Raccuglia, Suárez-Grimalt, et al. 2022). dFB neurons are thought to be sleep-promoting neurons as their activation reduces arousability and induces sleep, while inactivation causes insomnia (Pimentel et al. 2016; Suárez-Grimalt and Raccuglia 2021). On the other hand, helicon cells respond to visual stimuli (Shafer and Keene 2021).

dFB neurons are inhibited by wake-promoting dopaminergic neurons (Q. Liu et al. 2012), which mediate dopamine-induced changes within dFB neurons, including modulations of passive membrane properties, as well as voltage-dependent and leak potassium conductances (Pimentel et al. 2016). Activity of dFB neurons changes across the day, with increased activity observed at night (Raccuglia, Suárez-Grimalt, et al. 2022). Similar increase in activity has also been reported during sleep deprivation (Pimentel et al. 2016). The increase of the activity in dFB has been linked to the activity-dependent accumulation of ROS. While these neurons increase their activity at night and following sleep deprivation (Raccuglia, Suárez-Grimalt, et al. 2022), they remain silent in rested flies (Pimentel et al. 2016). dFB neurons inhibit helicon cells, which in turn are interconnected with R5 neurons (Suárez-Grimalt and Raccuglia 2021; Raccuglia, Suárez-Grimalt, et al. 2022; Shafer and Keene 2021). Thus, reduced activity of dFB during daytime might facilitate processing of visual information, while suppressing it at night via inhibition of the helicon cells. As the absence of sensory input may promote synchronization (Raccuglia, Suárez-Grimalt, et al. 2022), inhibition of helicon cells via dFB might promote SWA in R5 cells.

Both above-mentioned pathways converge in R5 neurons. **How might the interplay between these circuits modulate sleep–wakefulness in *Drosophila*?** It has been shown that optogenetic activation of TuBu neurons increases the amount of sleep in *Drosophila* (Lamaze et al. 2018), while activation of dFB neurons reduces locomotion (Raccuglia, Suárez-Grimalt, et al. 2022). Taken together, TuBu mediated R5 activation might induce sleep, whereas dFB may facilitate sleep via filtering out sensory inputs.

Apart from the above-mentioned populations, other networks and cell types also have been reported to be involved in *Drosophila* sleep regulation. Mushroom Body (MB), which is involved in olfactory memory, has been shown to contain both wake- and sleep-promoting neu-



rons (Suárez-Grimalt and Raccuglia 2021; Dubowy and Sehgal 2017). Furthermore, glial cells, which recently have been shown to integrate both circadian and homeostatic processes (Dopp et al. 2024), although the exact function of glia in *Drosophila* sleep regulation is not well-understood. Furthermore, ventral lateral neurons (LNvs) and dorsal lateral neurons (LNds), which are clock neurons responsible for, correspondingly, day and evening activity in *Drosophila*, influence the phase of diurnal  $\text{Ca}^{2+}$  level oscillations in R5 neurons (Andreani et al. 2022; Liang et al. 2019).

Interestingly, a recent genetic study which investigated how gene expression levels correlate with circadian and homeostatic processes identified two additional subclusters of EB ring neurons, apart from R5, showing a high number of genes correlating with homeostasis (Dopp et al. 2024).

Finally, sleep-wakefulness is also potentially regulated by other circuits mediating hunger, sexual arousal, or social interactions (Suárez-Grimalt and Raccuglia 2021; Shafer and Keene 2021).

### **1.2.3 Role of R5 neurons in *Drosophila* sleep**

As presented in the previous section, the activity of R5 neurons is modulated by circadian rhythm, homeostatic process, as well as sensory input. This section summarises findings regarding processes and behaviour modulated by R5 neurons, and their role in sleep in *Drosophila*.

Activation of R5 neurons reduces locomotion and increases sleep amount and depth (associated with increased homeostatic sleep drive) even in rested flies (Raccuglia, Suárez-Grimalt, et al. 2022; Sha Liu et al. 2016). However, inactivation of these neurons via inhibition of neurotransmitter release reduced rebound sleep and sleep depth only for sleep-deprived flies, without affecting baseline sleep (Sha Liu et al. 2016). Additionally, increased expression of Bruchpilot (BRP) protein, which is important for activity-dependent plasticity, has been reported in R5 neurons following sleep deprivation (Sha Liu et al. 2016). Notably, such an increase was not observed for other neurons in *Drosophila* brain. Furthermore, among EB ring neurons, a high number of genes correlated with sleep drive were found specifically in R5 neurons, while few or none were detected in other EB ring neuron clusters (Dopp et al. 2024). These suggest that R5 neurons are a central component of the sleep homeostat in *Drosophila*.

It has been suggested that SWA is generated at the level of R5 neurons (Raccuglia, Huang, et al. 2019), and R5 facilitates SWA in helicon cells (Raccuglia, Suárez-Grimalt, et al. 2022). Across different species, SWA have been associated with sleepiness, sleep quality, arousability threshold during sleep, as well as filtering sensory information during sleep (Suárez-Grimalt and Raccuglia 2021; Raccuglia, Huang, et al. 2019; Raccuglia, Suárez-Grimalt, et al. 2022). SWA has been proposed to have same role and effect in *Drosophila*. Furthermore, R5 neurons have been proposed to be functionally similar to TC cells in mammals. Similar to TC cells, R5 neurons switch their activity pattern from tonic spikes to bursting with increasing sleep need and following sleep deprivation, promote transition to sleep, and act as a sensory gate, increasing the arousability threshold during sleep while allowing a strong stimulus to induce the behavioural response (Suárez-Grimalt and Raccuglia 2021; Raccuglia, Huang, et al. 2019; Raccuglia, Suárez-Grimalt, et al. 2022; Yan et al. 2023; Gent et al. 2018).

How can the R5 neuron gate visual information and facilitate the reduction of locomotion? The previous section focused on networks that modulate R5 activity. R5 neurons, in turn, project to other neurons, including helicon and EPG cells. EPG cells represent the fly's heading direction and are involved in navigation (Raccuglia, Suárez-Grimalt, et al. 2022). They also receive excitation from helicon neurons, whose activation leads to increased activity of EPG neurons and increased locomotion (Raccuglia, Suárez-Grimalt, et al. 2022). Furthermore, EPG cells were found to be more responsive to visual stimulation during the day in comparison to night (Raccuglia, Suárez-Grimalt, et al. 2022). It has been shown that R5 and helicon cells modulate EPG activity in a reciprocal manner: stimulation of helicon cells depolarizes EPG neurons and promotes locomotion, while activation of R5 neurons hyperpolarizes EPG cells and reduces locomotion (Raccuglia, Suárez-Grimalt, et al. 2022). Thus, the dFB-helicon-R5 network can induce quiescence with increased sleep need via dFB-mediated suppression of visual information in helicon cells. dFB-mediated reduction of helicon activity at night could allow R5 neurons to override helicon drive to EPG, thereby reducing its activity and, consequently, locomotion (Raccuglia, Suárez-Grimalt, et al. 2022).

#### 1.2.4 Circadian and homeostatic regulation of R5 intrinsic properties

As stated in the previous section, it is thought that SWA is generated within EB R5 neurons. Differences between R5 activity during day- and nighttime, as well as following sleep deprivation, might result from circadian and homeostatic regulation, both of the R5 modulatory circuits, and of R5 neurons themselves. If SWA is generated at the level of R5 neurons, then when focusing on the R5 network, inputs from R5 modulatory circuits can be modelled as a constant input current. In this framework, the transition between R5 activity states could be modelled by modulating the magnitude of this input current, in combination with circadian and homeostatic modulations of the intrinsic properties of R5 neurons.

It has been reported that with increased sleep need, R5 neurons show increased firing rate, (Raccuglia, Huang, et al. 2019; Sha Liu et al. 2016), switch from tonic firing to bursting, synchronise and increase delta-power (0.5-1.5 Hz) (Raccuglia, Huang, et al. 2019). Additionally, the resting membrane potential of R5 neurons has been reported to be at more depolarized levels in sleep-deprived flies compared to control animals (Sha Liu et al. 2016). Several studies have reported molecular and cellular changes in R5 neurons in response to elevated sleep pressure.

**Cytosolic  $\text{Ca}^{2+}$  concentration.** Reversible increase in cytosolic  $\text{Ca}^{2+}$  levels has been observed in *Drosophila* R5 neurons in the morning, evening, and following sleep deprivation (Andreani et al. 2022; Sha Liu et al. 2016). Cytosolic  $\text{Ca}^{2+}$  levels can be modulated by several mechanisms. First, by activation of Inositol-triphosphate receptors (IP3Rs), which are intracellular  $\text{Ca}^{2+}$  channels located on the endoplasmic reticulum (ER) (Schmitz, Takahashi, and Karakas 2022). IP3R-mediated calcium release into cytosol within the cell can, in turn, trigger gene expression (Schmitz, Takahashi, and Karakas 2022), and  $\text{Ca}^{2+}$ -dependent synaptic plasticity (Sha Liu et al. 2016). IP3Rs regulation itself has been hypothesized to play a role in circadian clock entrainment in mammals (Hamada et al. 1999). Second, cytosolic  $\text{Ca}^{2+}$  levels can also be increased by activation of  $\text{Ca}^{2+}$  channels. It has been shown that T-type  $\text{Ca}^{2+}$  channels that are present in *Drosophila* presynaptic terminals are more active during the night in comparison to day (private discussion with David Oswald). Thus, increased neuronal activity during night and sleep deprivation could also explain the rise in cytosolic  $\text{Ca}^{2+}$  levels. To my knowledge, whether the increase in calcium concentration is a cause or a consequence of increased neuronal activity and bursting in R5 neurons is unknown. However, both processes might modulate cytosolic

Ca<sup>2+</sup> level in *Drosophila* R5 neurons.

**Gene expression.** Expression of the gene encoding potassium EAG channel has been observed to negatively correlate with sleep drive in R5 neurons (Dopp et al. 2024). Taking into account that  $K^+$  currents hyperpolarize the membrane, an elevated number of EAG channels may oppose depolarizing currents, thereby reducing excitability and preventing transition to the bursting state.

**Modulation within presynaptic terminals.** Furthermore, BRP levels have been reported to increase only in R5 neurons following sleep deprivation (Sha Liu et al. 2016). BRPs are localized at presynaptic terminals (Wagh et al. 2006), and elevated BRP level has been associated with promotion of high-voltage activated Ca<sup>2+</sup> channel density (Kittel et al. 2006). Strikingly, neither morning nor evening sleep deprivation induced considerable changes in gene expression (Andreani et al. 2022). These results may reflect a process called synaptic remodelling, where existing synapses are eliminated to form new synapses on different dendritic or axonal branches (Kurup and Jin 2016). Alternatively, this absence of the effect may have been influenced by experimental conditions or methodological limitations.

## 1.3 Bursting

### 1.3.1 Onset and offset of bursts

Bursting in neurons is characterized by transition of the neuron between two states: 1) **resting state**, where the neuron does not fire action potentials and 2) **spiking state** (Fig. 3, bottom). Over the time course, the bursting neuron switches between the two states, resulting in the periods of quiescence (i.e. inactivity, or resting) and high-frequency spiking.

Generally, bursting is thought of as an interplay between oscillations with fast and slow timescales (referred to as **fast-slow subsystems**). Fast timescale is related to the spiking within a burst, while the slow timescale is associated with modulation of the transition between spiking and resting states (Izhikevich 2006). What cellular mechanisms may cause burst initiation and termination? These mechanisms underlying fast-slow dynamics can generally be divided into four classes based on the underlying processes responsible for burst initiation and termination, as summarized by Izhikevich (Izhikevich 2006) (see also Figure 3). In the following, the main

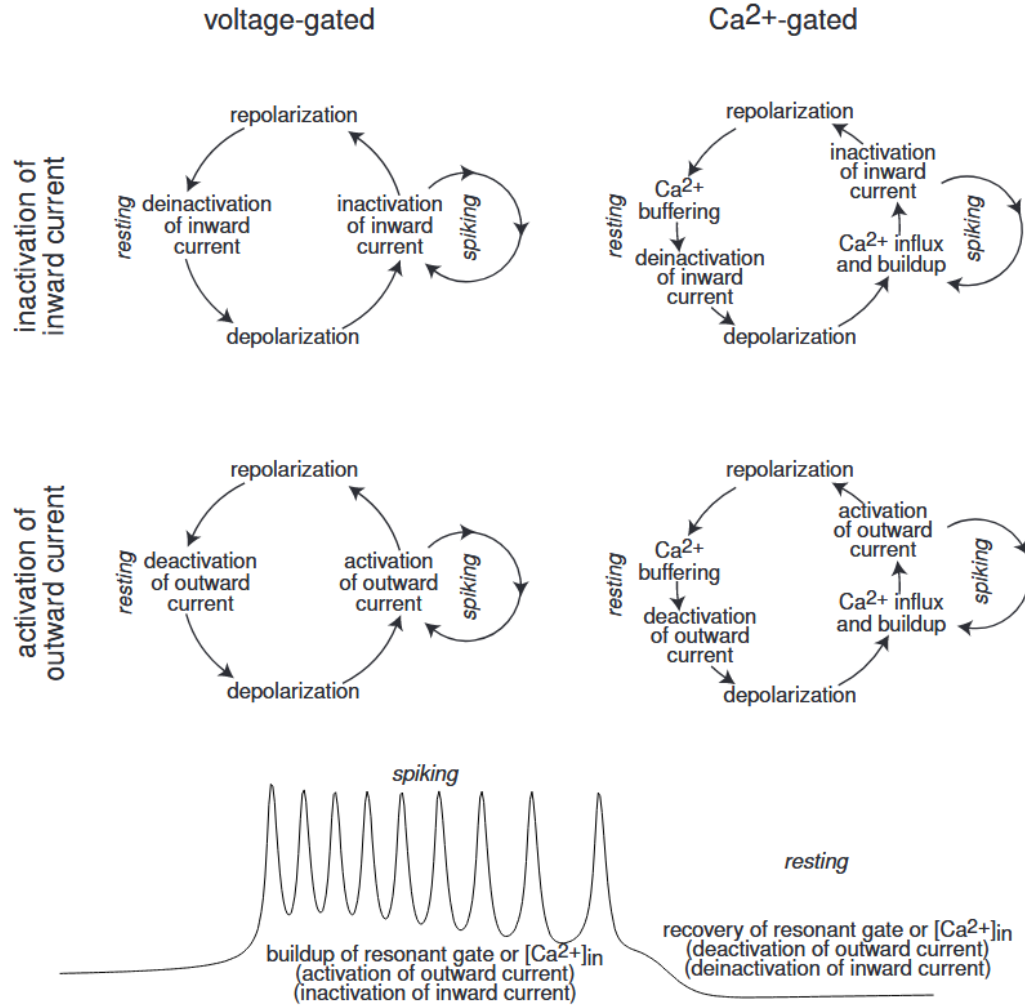


**Figure 3: Cellular mechanisms of burst generation.** Top: four mechanisms of burst generation based on the fast-slow decomposition. Bottom: effects of currents on the transition between spiking and resting states. For details, see the main text. Figure adapted from (Izhikevich 2006), with modifications.

principles behind these mechanisms will be outlined.

Mechanism of the burst termination might involve either voltage and/or  $\text{Ca}^{2+}$  dependent hyperpolarizing currents. The onset and offset of the spiking phase can be caused by inward and/or outward currents. Inward currents are depolarizing currents (mostly mediated by sodium ( $\text{Na}^+$ ) and calcium ( $\text{Ca}^{2+}$ ) ions) driving the membrane potential towards the spiking threshold. Outward currents, on the other hand, are hyperpolarizing currents, effectively increasing spiking threshold and are mostly mediated by potassium ( $\text{K}^+$ ) ions. The onset (offset) of the burst can thus be caused by deinactivation (inactivation) of inward currents, or deactivation (activation) of

outward currents. Deactivation of inward currents requires the corresponding ion channel to have an inactivation gate, where deactivation refers to the removal of inactivation, i.e. opening of the inactivation gate.

Furthermore, the termination of a burst can be caused by ion channels which mediate hyperpolarizing currents and whose activation depends on the intracellular calcium concentration. Calcium entry can lead to activation of  $\text{Ca}^{2+}$ -dependent outward currents, or inactivation of  $\text{Ca}^{2+}$ -dependent inward currents. This, in turn, promotes the dominance of outward currents, driving the membrane potential to more negative values and thus contributing to spike termination.

Within the scope of the current thesis, it is investigated whether bursting for *Drosophila* R5 neurons depends on  $\text{Ca}^{2+}$  channels. The possible bursting mechanism mediated by T-type channels will be discussed in more detail in Section 1.3.2. Shortly, in bursting models, where onset and offset of the bursts are mediated by slowly inactivating (e.g. T-type  $\text{Ca}^{2+}$ ) channels, the transition between spiking and resting states occurs, correspondingly, via deactivation and inactivation of these channels (upper left diagram in Figure 3).

### **1.3.2 Ion channel contributions in bursting and under sodium channel blockade**

Although the cellular mechanisms of spiking and bursting have not been investigated in *Drosophila* R5 neurons, and also little is known about ion channels expressed in these neurons, numerous experimental and computational studies have investigated the effects of ion channels in burst generation in other neuronal types in various animal species. These include LNvs neurons in *Drosophila*, as well as bursting neurons in rodents (Vickstrom et al. 2020; Golomb, Yue, and Yaari 2006; Shaolin Liu and Shipley 2008; Wang 1994; McCormick and Huguenard 1992). Understanding the bursting mechanism of other models might provide an insight into which ion channels might contribute to burst firing in *Drosophila* R5 neurons. The following section summarizes ion channels reported to contribute to bursting activity in various animal species and describes their roles in shaping the burst dynamics.

#### **T-Type and HCN channels**

T-Type and Hyperpolarization-activated Cyclic Nucleotide-gated (HCN) channels have been found to be important components for many bursting neurons in various animal species (Amar-

illo et al. 2014; Vickstrom et al. 2020; A. Destexhe and Babloyantz 1993), and taking part in subthreshold dynamics and slow oscillations (Wang 1994). For some neurons, they have been hypothesized and experimentally validated to play a substantial role in mediating bursting and low-threshold  $\text{Ca}^{2+}$  spikes after sodium channels are blocked in the experimental conditions McCormick and Huguenard 1992; Shaolin Liu and Shipley 2008; Vickstrom et al. 2020; Suzuki and Rogawski 1989. T-type channels are voltage-gated calcium channels that activate fast at hyperpolarized membrane potentials, inactivate slowly at potentials larger than the firing threshold, and deinactivate at hyperpolarized membrane potentials. HCN channels generally have only an activation gate that opens with hyperpolarization. They mediate depolarizing current (A. Destexhe and Babloyantz 1993), and facilitate setting the minimal membrane potential (e.g. during oscillations) at more depolarized potentials (Shaolin Liu and Shipley 2008).

The mechanism of bursting that is mediated by T-type- and h-currents has been described previously (see e.g. (Shaolin Liu and Shipley 2008; Wang 1994)). In these models, hyperpolarizing current activates HCN channels that, once opened, depolarize the membrane until the activation threshold of T-type channels. When T-type channels open, they provide an excitatory current driving the neuron into a spiking state. At higher potentials, T-type currents slowly inactivate, and once inactivation is sufficiently large, the hyperpolarizing currents take over to drive the membrane potential back to a hyperpolarized state. At these potentials, T-type channels deinactivate and HCN channels activate, and the cycle repeats. Such bursting, when a neuron bursts due to hyperpolarizing current, is referred to as **inhibition-induced bursting** (Izhikevich 2006).

H current has been shown to increase burst frequency (Shaolin Liu and Shipley 2008; McCormick and Huguenard 1992). Furthermore, it has also been associated with afterhyperpolarization (AHP) (undershoot of membrane potential below resting membrane potential (McCormick and Huguenard 1992), e.g. Figure 4 top right plot). For example, for some neurons, reduction of AHP amplitude has been reported with increasing blockade of HCN channels (Oswald et al. 2009; Bonin et al. 2013). However, it is worth noting that HCN channels are not necessary for inhibition-induced bursting, or for AHP. For example, within the scope of this thesis, simulations of the bursting model described in (Wang 1994) demonstrated that persistent sodium leak, potassium and T-type channels are necessary and sufficient to generate bursting

behaviour within the investigated parameter regime. Furthermore, the undershoot depends on the dynamical properties of the system, as it will be discussed in more detail in Section ??.

### **L-Type channels**

Another  $\text{Ca}^{2+}$  channels that could be involved in bursting are the L-type channels. Similar to T-type channels, they are characterized by slow inactivation, however, they are activated at higher membrane potentials (Shaolin Liu and Shipley 2008). These channels have been shown to mediate low-voltage activated (LVA)  $\text{Ca}^{2+}$  currents and increase the burst duration in mice periglomerular cells (Shaolin Liu and Shipley 2008) and *Drosophila* motoneurons (Kadas et al. 2017). Although it is not yet known whether *Drosophila* R5 neurons express L-type channels, they are potential candidates to be involved in the modulation of bursting in these cells.

### **Sodium channels**

Persistent sodium channels have been shown to modulate the number of spikes within a burst. Specifically, for several computational and biological models, increasing the maximal conductance of these channels increased the number of spikes per burst (Shaolin Liu and Shipley 2008; Golomb, Yue, and Yaari 2006).

As bursting with one spike per burst can be thought of as tonic firing, modulation of persistent sodium channels can be a potential mechanism to switch from tonic to bursting behaviour in *Drosophila* R5 neurons.

### **Potassium channels**

As in neurons reversal potential of potassium is generally found to be at much negative potentials than the resting membrane potential (see e.g. Table 1), they generally counteract depolarizing currents and result in reduction of neuronal response to such currents (McCormick and Huguenard 1992). Depending on their activation threshold and dynamic properties, they can influence subthreshold and/or spiking activity. For example, transient potassium current has been proposed to modulate the initial phase of LVA calcium spikes (Huguenard and McCormick 1992) and reduce the firing rate of a neuron (McCormick and Huguenard 1992). In contrast, another voltage-gated potassium current, characterized by slower activation and inactivation kinetics (corresponding ionic current referred to as  $I_{K2}$ ), has been suggested to influence the later phases of LVA  $\text{Ca}^{2+}$  spikes (Huguenard and McCormick 1992), while also contributing to decreased neuronal firing rate (McCormick and Huguenard 1992).



Another important potassium channel is the large-conductance  $\text{Ca}^{2+}$  activated potassium channel (referred to as the BK channel). Activation of these channels may require the simultaneous presence of depolarization and calcium influx. Due to their large conductance, it has been proposed that BK channels might contribute to the termination of the burst, thus regulating the burst duration (Shaolin Liu and Shipley 2008).

### **Leak Channels**

Leak channels predominantly modulate resting membrane potential (McCormick and Huguenard 1992; Amarillo et al. 2014). The parameters for these channels (maximal conductance and reversal potential) are often tuned to reproduce experimentally observed resting membrane potential and input resistance (Wang 1994).

### **$\text{Ca}^{2+}$ Concentration**

Intra- and extracellular  $\text{Ca}^{2+}$  concentration has been shown to also modulate bursting behaviour. While intracellular calcium buffering has been shown to stabilise bursting activity, as well as resting membrane potential (Shaolin Liu and Shipley 2008), decreasing extracellular  $\text{Ca}^{2+}$  concentration can switch from spiking to bursting activity (Golomb, Yue, and Yaari 2006).

How can the R5 neuron switch from tonic to bursting activity? As it was stated above, modulation of the number of persistent sodium channels (which will affect the maximal conductance at the population level), as well as a decrease in extracellular calcium concentration, can induce bursting. It has been demonstrated that the same could be achieved by modulation of maximal conductances of voltage-gated transient- and calcium-gated potassium channels (Franci, Drion, and Sepulchre 2018). Generally, as potassium channels modulate the excitability of the cell (Brüggemann et al. 1993), switching from bursting to tonic activity could potentially be achieved by increasing the maximal conductance of other voltage-gated potassium channels. As it was outlined in Section 1.1.2, a potential candidate is the potassium EAG channel. However, it is important to note, that this might not be straightforward, as computational study of McCormick and Huguenard showed that in their model decrease in any of the voltage-dependent potassium currents increased other voltage-gated potassium currents (McCormick and Huguenard 1992).

It is important to keep in mind that it is unknown whether R5 neurons exhibit inhibition-induced bursting or whether hyperpolarization-activated depolarizing currents are involved in

bursting activity. A neuron can also burst tonically following depolarizing current, or exhibit bursting after removal of inhibitory current (inhibition-rebound bursting) (Izhikevich 2006) (see also Figure ??). To my knowledge, there is no published experimental observation regarding this matter.

Secondly, even if the bursts in R5 neurons are mediated by T-type channels, the contribution of specific ion channels might depend on the properties of the whole dynamical system. Several examples will be presented in the rest of this section.

It has been shown that elevated maximal conductance of T-type channels increases burst duration and decreases period of bursting (Park, Rubchinsky, and Ahn 2021). Furthermore, the maximal conductance of those channels has been reported to positively correlate with the resting membrane potential (Amarillo et al. 2014). However, the model presented in (Amarillo et al. 2014) did not contain calcium-gated potassium channels. Because the latter mediates hyperpolarizing current, a reduction in the influx of calcium through calcium channels might induce reduced activation of such potassium channels. This might effectively lead to an increase in resting membrane potential instead of the expected decrease due to the depolarizing nature of T-type currents.

Furthermore, although for some models persistent sodium channels are necessary to induce bursting (see e.g. (Shaolin Liu and Shipley 2008; Wang 1994)), for other models these channels are neither necessary nor sufficient to induce bursting (see e.g. (Golomb, Yue, and Yaari 2006)).

Such differences in modulatory effects can be observed not only between different models but also within the same model operating in different parameter regimes. For example, altering a single parameter may result in an increase or decrease in the number of spikes per burst, depending on the values of the chosen fixed parameters.

## **1.4 Experimental Findings and Mechanistic Proposals**

### **1.4.1 Blocking of $Na$ and T-Type $Ca^{2+}$ Channels in R5 Neurons**

#### **Bursting**

T-type  $Ca^{2+}$  channels have been shown to mediate bursting activity in many neurons, regardless of animal species (see Section 1.3.2), including mammalian TC cells. *Drosophila* homologe

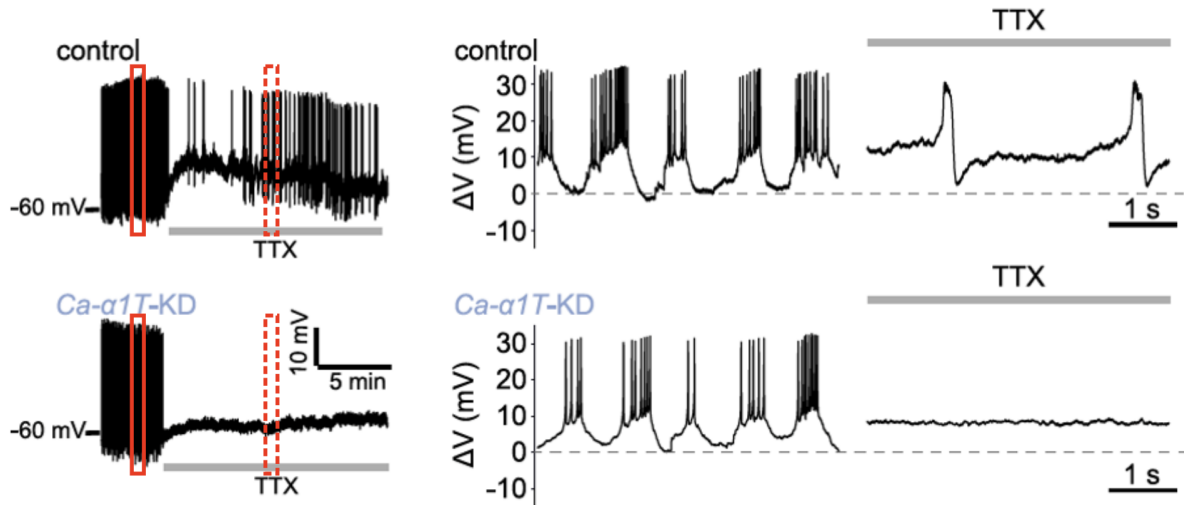


**Figure 4: Voltage traces in control and *Ca-α1T*-KD flies following block of sodium channels.** Left: recorded voltage traces obtained by **patch-clamp** recordings of R5 neurons from **sleep-deprived** control (top) and T-type channel knockdown (bottom) flies. Middle: Recorded voltage traces from the region outlined by the solid red rectangle in the left plots (before application of Tetrodotoxin (TTX)); 0 on the  $\Delta V$  axis accounts for the mean resting membrane potential (+ corrected for Liquid Junction Potential (?)) Maybe that is why in contrast to Figure 5) the trough on the left plot seems to be lower for *Ca-α1T-KD* than for control. Right: Recorded voltage traces from the region outlined by the dashed red rectangle in the left plots (after application of TTX). The image displays unpublished data provided by David Oswald and Anatoli Ender.

for mammalian T-type  $\text{Ca}^{2+}$  channels has also been identified (Jeong et al. 2015). As correspondence between R5 and TC cells has been suggested, a natural question to ask would be whether and to what extent T-type channels contribute to bursting in *Drosophila* R5 neurons.

An unpublished study by **David Oswald and Anatoli Ender** has revealed that **T-type channels in R5 neurons are expressed at presynaptic sites**. Patch-clamp recordings from R5 neurons of sleep-deprived flies exhibited bursting activity (Figure 4 top). Blocking *Na* channels with TTX resulted in oscillations with pronounced AHP and lower frequency (**exact value**) in comparison to 1 Hz interburst frequency (defined by time period between first spike in the current burst and last spike in the preceding burst) before TTX application (Figure 4, top).

Next (**using which tools?**) Oswald and colleagues knocked down T-type calcium channels in *Drosophila* R5 neurons (labelled as *Ca-α1T*-KD flies) (Figure 4, bottom). Interestingly, T-type  $\text{Ca}^{2+}$  knockdown (KD) fly R5 neurons still retained bursting activity, with the same intraburst frequency (frequency of the spikes within the burst, Figure 5, left). Strikingly, the resting mem-

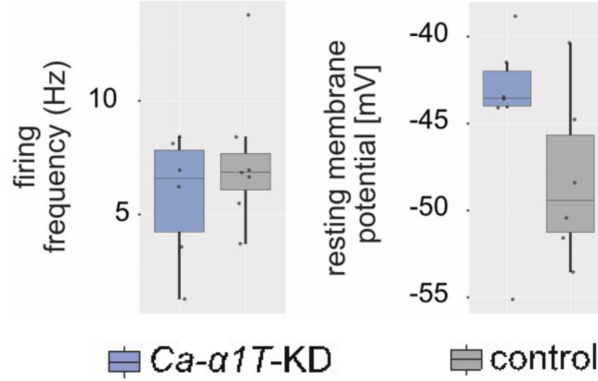


**Figure 5: Firing rate and resting membrane potential after  $\text{Na}^+$  block in control and *Ca-α1T-KD* flies.** Comparison of firing rate and resting membrane potential between T-Type channel knockdown and control flies before TTX application. The corresponding voltage traces are given in Figure 4. The image displays unpublished data provided by David Oswald and Anatoli Ender.

brane potential was higher for *Ca-α1T-KD* flies in comparison to the control ones. At first sight, this result seems counterintuitive, as  $\text{Ca}^{2+}$  currents are depolarizing currents (rising membrane potential towards spiking threshold). Indeed, simulation studies of TC cells have reported a reduction in resting membrane potential following the blockade of T-type  $\text{Ca}^{2+}$  channels (Amarillo et al. 2014). *Ca-α1T-KD* flies oscillatory activity diminished after TTX application, suggesting a role for the T-type calcium current in generating those oscillations.

Why is bursting retained, and why is an increase in resting membrane potential observed after T-type  $\text{Ca}^{2+}$  channel blockade, is not well-understood. One possible explanation for the retention of bursting activity is that a subset of T-type channels may remain functional after *Ca-α1T* knockdown. The remaining calcium current could be sufficient to depolarize the membrane potential to the spiking threshold and support bursting, however, insufficient to sustain oscillatory activity following *Na* channel blockade. Alternatively, other ion channels that conduct depolarizing currents (other than *Na* and *T-type*  $\text{Ca}^{2+}$  channels) might contribute to bursting. A potential candidate is high-voltage activated (HVA)  $\text{Ca}^{2+}$  current mediated by L-type calcium channels. As described in Section 1.3.2, L-type channels are characterized by slow inactivation, similar to the T-type  $\text{Ca}^{2+}$  channels. Thus, instead of T-type channels, bursting can potentially be mediated by L-type channels.

As discussed in Section 1.3.2, an increase in the resting membrane potential following block-

ade of T-type  $\text{Ca}^{2+}$  channels might be an indication of the calcium-gated potassium channels. If the conductance of these potassium channels is greater than that of the T-type channels, blocking T-type channels could effectively cause an increase in the resting membrane potential by reducing the activation of  $\text{Ca}^{2+}$ -gated  $\text{K}^{+}$  channels. Indeed, in some modeling studies, the maximal conductance of  $\text{Ca}^{2+}$  gated  $\text{K}^{+}$  channels are set to be at least an order of magnitude larger than that of the T-type  $\text{Ca}^{2+}$  channels (Franci, Drion, and Sepulchre 2018; Nowotny, Levi, and Selverston 2008). However, it should be noted that other modeling studies have used the maximal conductance of  $\text{Ca}^{2+}$  gated  $\text{K}^{+}$  channels to be either only about twice as large (Alonso and Marder 2019), or even smaller (Park, Rubchinsky, and Ahn 2021), compared to that of T-type channels. Alternatively, the observed depolarization could result from a more complex mechanism, potentially mediated by  $\text{Ca}^{2+}$ -dependent synaptic plasticity.

### **Slow oscillations after $\text{Na}^{+}$ channel blockade**

Another interesting observation in the above-mentioned experiments is the presence of slow oscillations in membrane potential after blockade of  $\text{Na}^{+}$  channels in control flies, which are abolished in T-Type KD animals (Figure 4, right column). The oscillations in the control animals are characterized by apparent AHP,  $\sim 100\text{ms}$  width spikes, and relatively large period on the order of several seconds. Which processes that mediate these slow oscillations are not well understood.

What may the potential mechanisms be? Since the oscillations are abolished following T-type calcium channel knockdown, the depolarization phase may be mediated by these channels. However, the involvement of T-type calcium channels in generating the depolarizing current does not necessarily imply that they are responsible for the long interspike intervals. In fact, the gating kinetics of these channels are relatively fast, on the order of a few hundred milliseconds (see Section ??? for details on T-type channel modeling).

Other ion channels with larger time constants may contribute to the large interspike interval. However, it is important to note that the timescale of oscillations may not be determined solely by the kinetics of the gating variables. As discussed in Section 1.1.1, the ion flow through the channels can also be modulated by ligands. For example, BK channels, which are characterized by large conductance, are activated by both membrane depolarization and intracellular calcium. This has two implications. First, activation of BK channels requires both membrane depolariza-

tion and increased calcium concentration. Second, if these channels are partially open at rest, the gradual removal of calcium following an action potential may lead to their slow inactivation.

In many bursting models, calcium removal is either neglected (see e.g. (Wang 1994; Amarillo et al. 2014)), or assume to have relatively fast time constant ranging between 1-15 milliseconds (see e.g. (McCormick and Huguenard 1992; Golomb, Yue, and Yaari 2006; Alonso and Marder 2019; Park, Rubchinsky, and Ahn 2021)). However, experimental studies have reported two distinct timescales of calcium decay in single nerve terminals following single action potentials of rat pyramidal cells (Koester and Sakmann 2000), with a fast (10ms) and slow component on the order of several hundred milliseconds.

Thus, slow ion dynamics may also effectively regulate the timescale of oscillations.

#### 1.4.2 Transition between tonic and bursting activity

R5 neurons synchronize and exhibit bursting activity with increasing sleep need (Raccuglia, Huang, et al. 2019; Sha Liu et al. 2016) (Figures 6-8). Study of Raccuglia and colleagues showed that delta power (0.5-1.5Hz) of the compound R5 oscillations increases progressively throughout the day, peaks during the night when the fly displays consolidated sleep, and subsequently declines toward the morning (Raccuglia, Huang, et al. 2019) (Figure 6 right). The delta power of the compound SWA was observed to be even stronger for sleep-deprived flies (Figure 6 left).

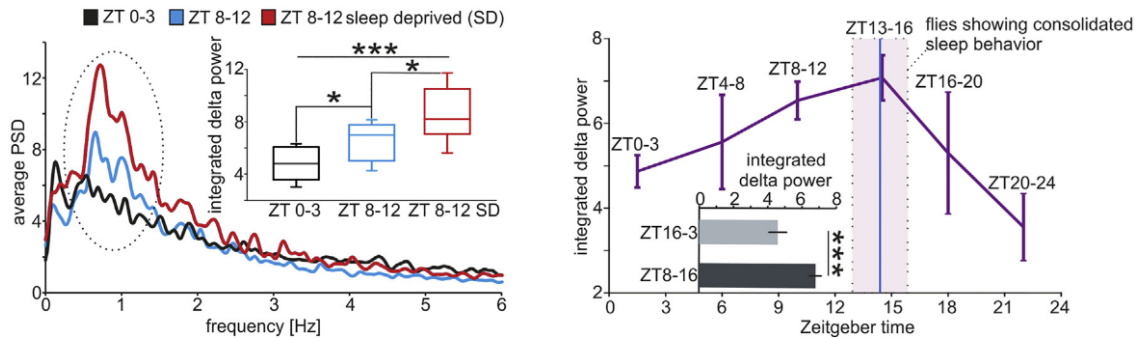


**Figure 6: Diurnal variation of R5 compound SWA power spectrum.** Left: Power Spectral Density (PSD) of voltage recordings representing compound R5 activity at different Zeitgeber time (ZT) times, averaged over trials. The delta frequency range (0.5-1.5Hz) is outlined by the dashed circle. Right: variation of the average delta power throughout the day. The delta power increases throughout the course of the day, reaching its peak at night, during consolidated sleep. The average PSD is even higher in sleep-deprived flies. Adapted from (Raccuglia, Huang, et al. 2019)

Furthermore, Liu and colleagues reported an increase in firing rate of R5 neurons at early night, in comparison to early morning (Sha Liu et al. 2016), and being highest for sleep-deprived flies (Figure 7).

The compound  $\sim 1$  Hz SWA in R5 originates from the synchronization between individual R5 units, which display a similar peak in the power spectrum as observed in compound oscillations (Raccuglia, Huang, et al. 2019) (Figure 8). In contrast, during daytime, the peak in the delta power is observed neither in the compound SWA (Figure 6 left) nor in the single-cell activity (Figure 8 left). Furthermore, during the day, the R5 neurons exhibit tonic firing rate (Figure 7).

Transition from tonic to bursting activity, and increased power in the compound SWA has been associated with reduced locomotion, increased sleep drive, sleep depth, and filtering of the sensory information during sleep (Sha Liu et al. 2016; Raccuglia, Huang, et al. 2019; Raccuglia, Suárez-Grimalt, et al. 2022; Suárez-Grimalt and Raccuglia 2021). However, how individual R5 neurons switch from tonic spiking to bursting is not well understood.

Generally, the neurons which exhibit inhibition-induced bursting can fire tonically if an ex-

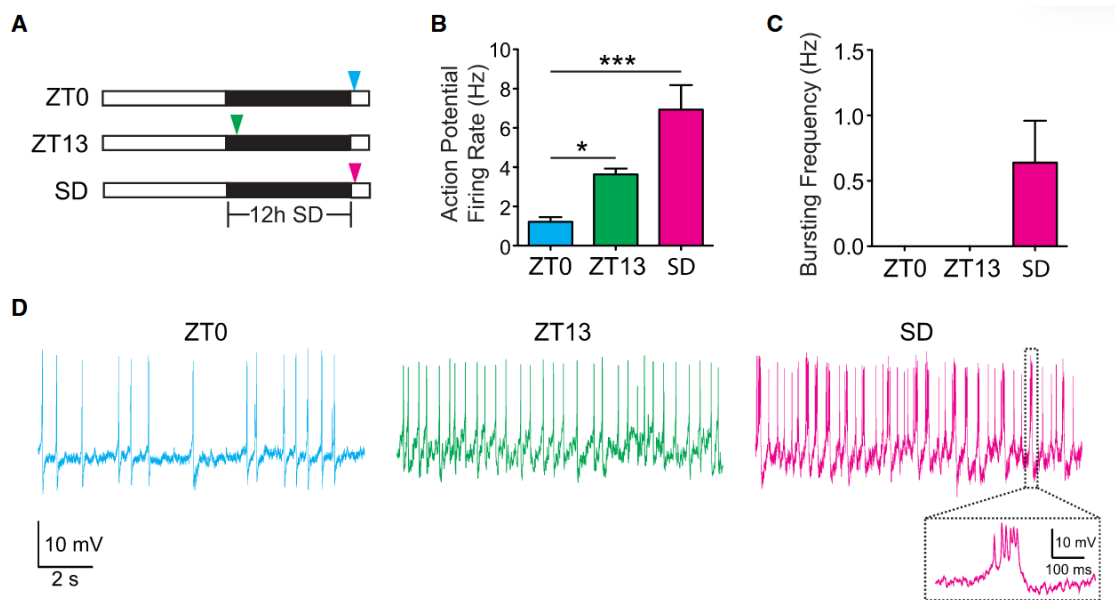


**Figure 7: Diurnal variation of R5 single-cell voltage trace.** (A) Time points when recordings were made. SD = sleep deprivation (B) Firing rates and (C) bursting frequency of R5 neurons at different times of the day. (D) Examples of recorded voltage traces. Bursting was observed only in sleep-deprived flies. Adapted from (Sha Liu et al. 2016)

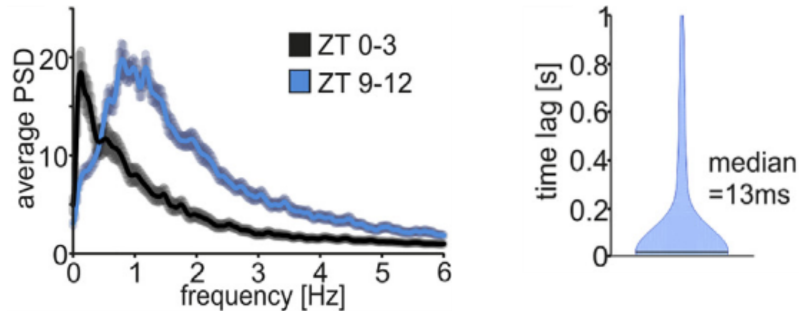


**Figure 8: Contribution of individual R5 neurons in compound SWA** Left: Average power spectrum of R5 single-cell SWA. Right: Pair-wise time lag distribution of depolarization phases between individual R5 neurons recorded at ZT 9-12. Adapted from (Raccuglia, Huang, et al. 2019)

citatory current is injected (see e.g. (Wang 1994)). In the case of excitatory drive, the neuron is driven in the spiking state by constant input current by direct activation of the fast-subsystem, rather than transition to the spiking state via T-type  $\text{Ca}^{2+}$  channels. However, in this case, the tonic firing rate is comparable to the firing rate within the bursts. Contrary, R5 neurons exhibit low-frequency tonic firing (Raccuglia, Huang, et al. 2019) (Figure 6). Thus, the switch from bursting to tonic activity for R5 neurons cannot be explained solely by a change in external drive. In these cells, the critical factor of the transition might be the reduced neuronal excitability in the tonic regime in comparison to the bursting state.

As discussed in Section 1.2.4, the change in activity can be caused by a combination of multiple factors, including changes in external drive and alterations in the intrinsic properties of R5 neurons. External modulation may occur through circadian and/or homeostatic regulation of R5 modulatory circuits(see Section 1.2.2), while intrinsic modulation may involve changes in the dynamical properties of R5 neurons. As presented in Sections 1.2.4 and 1.3.2, these mechanisms may involve 1) modulation of intracellular  $\text{Ca}^{2+}$  concentration within R5 neurons through IP3R-mediated calcium release from EB, 2)  $\text{Ca}^{2+}$ -dependent synaptic plasticity in R5, 3) modulated expression of potassium EAG channel, and 4) homeostatic/circadian system mediated changes in activity of R5 modulatory circuits, including increasing activation of R5 neurons via TuBu cells with prolonged wakefulness, or via helicon cells.



### 1.4.3 dFB mediated inhibition of helicon cells at night

It has been hypothesized that reduction of helicon activity could be mediated by helicon cells activating dFB neurons (Raccuglia, Suárez-Grimalt, et al. 2022). Since R5 and dFB neurons are not directly connected, modulation of dFB activity by R5 activation would require an additional, currently unidentified pathway, for example, via another neuron, or cell classes such as glial cells. It has been proposed that glial cells could influence neuronal excitability and synaptic transmission, and potentially coordinate activity across neuronal networks (Fields and Stevens-Graham 2002). Alternatively, as it was indicated in Section 1.2.2, activity of dFB neurons is inhibited by wake-promoting dopaminergic neurons. Consequently, inhibition of dFB during the day could result in the reduction of helicon inhibition by these neurons. In contrast, during night, dFB may be more active due to the removal of inhibitory input from the above-mentioned dopaminergic neurons, leading to the increased inhibition of helicon cells. Whether the activity of these neurons depends on R5 or if they are part of another pathway still should be investigated. In addition to modulation of dFB activity via wake-promoting dopaminergic neurons, dFB neurons also showed the highest number of genes (specifically, 121) whose expression level correlated with sleep drive (Dopp et al. 2024). However, the authors did not report whether or how those correlated genes could affect dFB activity. Taken together, inhibition of helicon cells may result from circadian modulation of dFB neurons rather than from R5-mediated mechanisms, as originally proposed in (Raccuglia, Suárez-Grimalt, et al. 2022). Overall, homeostatic and circadian regulation of dFB activity could represent an alternative or an additional mechanism for modulating helicon cell activity, ultimately functioning as a switch for sensory gating during sleep and wakefulness.

It is worth mentioning that optogenetic activation of R5 neurons led to presynaptic SWA in dFB neurons (Raccuglia, Suárez-Grimalt, et al. 2022). Because R5 and dFB are functionally connected via excitatory helicon cells, and R5 neurons may induce SWA in helicon cells (see Section 1.2.3), SWA in dFB neurons following R5 activation might result from helicon-dFB connection through R5-induced SWA in helicon cells.

#### 1.4.4 Delayed synchronization between R5 and helicon populations

**Unpublished, but is in Laura's Master Thesis.** Another intriguing result has been reported during the analysis of synchronization between R5 and helicon cells. During baseline sleep (i.e. without sleep deprivation), the time lagged correlation between R5 and helicon activity revealed two distinct synchronization modes: one with near-zero time lag, and another "shifted" state, when helicon preceded R5 activity by 50-200 ms (unpublished data from David Oswald and Anatoli Ender; see also (Krumm 2021)). Furthermore, sensory input to helicon cells has been thought to play an important role in the observed shifted state, as only near-zero time lag synchronization was observed in the ex vivo experiments.

It has been hypothesized that while R5 neuron entrains SWA in helicon cells during sleep, helicon cells, in turn, drive R5 activity during the day as a result of sensory input. The delay could, therefore, reflect the synaptic transmission delay between helicon and R5 neurons. Although the above-mentioned hypothesis accounts for the absence of the "shifted" state in ex-vivo experiments, it does not explain why both states have been observed at night despite reduced visual stimulation.

Alternatively, delayed synchronization between helicon and R5 cells during night and following sleep deprivation, with helicon cells preceding the dynamics, might be mediated by gap-junctions. R5 may excite helicon cells through gap-junctions and cause them to spike before R5 neurons reach spiking threshold themselves. This excitation will be more effective when helicon cells are more excitable, and/or R5 cells are more active. During normal sleep, increased activity of R5 neurons may induce spikes via gap-junctions in some helicon cells, while failing to do so in others. As R5 neurons increase delta power (0.5-1.5 Hz) following sleep deprivation (Raccuglia, Huang, et al. 2019), this increased activity may amplify gap-junction mediated excitation of helicon cells by R5 neurons. This may explain why only the delayed state was observed following sleep deprivation. Lastly, visual input might drive helicon cells to more excitable states, making it easier for R5 neurons to drive helicon cells. This aligns with the proposed hypothesis by Davide Raccuglia and colleagues, that a shifted state might result from interference with sensory input (unpublished study by Davide Raccuglia and colleagues).

## 1.5 Summary and Outlook

R5 neurons are modulated by both circadian and homeostatic processes. This modulation can be divided into two distinct mechanisms: 1) effective modulation via changing the activity of the R5 modulatory circuits, and 2) changes of cellular properties within R5 neurons themselves.

Assuming that SWA is generated intrinsically within R5 neurons, the external input current to R5 is proposed to be modeled as constant. Several mechanisms have been proposed to explain experimental observations:

1. Retaining of bursting following T-type channel knock-down may be explained by 1) partial blockade of T-type channels, or 2) involvement of other hyperpolarization-activated depolarizing ion channels, such as L-type channels;
2. Different mechanisms may be involved in transition between spiking and bursting in R5 neurons, including: (1) modulation of the mean current input to R5 neurons from circuits modulating R5 activity, (2) circadian modulation of intracellular calcium levels in R5 neurons, potentially mediated by IP3R-dependent calcium release from ER; (3)  $\text{Ca}^{2+}$ -dependent synaptic plasticity, (4) modulation in expression of potassium EAG ion channels within R5 neurons;
3. Slow oscillations in membrane potentials following  $\text{Na}^+$  channel blockade may be mediated not only by the slow kinetics of ion channel gating variables, but also by a slow rate of intracellular calcium removal, which can lead to gradual inactivation of calcium-activated potassium channels that oppose depolarization when active;
4. Increase in resting membrane potential following T-type channel knock-down may indicate involvement of calcium-gated potassium channels, which activate with increasing intracellular  $\text{Ca}^{2+}$  concentration, and thus mediate smaller current with reduced number of calcium channels;
5. Increased delta power following sleep deprivation may result from activity-dependent modulations (e.g. accumulation of ROS) within R5 neurons, or circuits affecting their activity, rather than from changes in ion channel expression or concentration.